Downloaded from genome.cshlp.org on November 17, 2026 . Published by Cold Spring Harbor Laboratory Press



A SNP panel for coanalysis of capture and shotgun ancient DNA data

Romain Fournier, Alice Pearson Fulton, Daniel Tabin, et al.

Genome Res. 2026 36: 1818-1824 originally published online August 12, 2026
Access the most recent version at doi:10.1101/gr.281262.125

References This article cites 33 articles, 6 of which can be accessed free at:
http://genome.cshlp.org/content/36/9/1818.full.html#ref-list-1

Creative Commons License This article is distributed exclusively by Cold Spring Harbor Laboratory Press for the first six months after the full-issue publication date (see https://genome.cshlp.org/site/misc/terms.xhtml). After six months, it is available under a Creative Commons License (Attribution-NonCommercial 4.0 International), as described at http://creativecommons.org/licenses/by-nc/4.0/.

Email Alerting Service Receive free email alerts when new articles cite this article - sign up in the box at the top right corner of the article or **click here.**



To subscribe to *Genome Research* go to:
https://genome.cshlp.org/subscriptions

© 2026 Fournier et al.; Published by Cold Spring Harbor Laboratory Press

Downloaded from genome.cshlp.org on November 17, 2026 . Published by Cold Spring Harbor Laboratory Press

Method

A SNP panel for coanalysis of capture and shotgun ancient DNA data

Romain Fournier,[1] Alice Pearson Fulton,[1] Daniel Tabin,[1] and David Reich[1,2,3,4]

[1]*Department of Human Evolutionary Biology, Harvard University, Cambridge, Massachusetts 02138, USA;* [2]*Department of Genetics, Harvard Medical School, Boston, Massachusetts 02115, USA;* [3]*Broad Institute of MIT and Harvard, Cambridge, Massachusetts 02142, USA;* [4]*Howard Hughes Medical Institute, Boston, Massachusetts 02138, USA*

Advances in technology have decreased the cost of generating genetic data from ancient people, resulting in exponentially increasing numbers of individuals with whole-genome data. However, these technologies come with platform-specific biases, limiting coanalyzability of individuals sequenced with different technologies as well as joint analysis of modern and ancient individuals. Here, we present a method to identify single-nucleotide polymorphisms (SNPs) with minimal technology-specific bias. Leveraging data from more than 18,000 individuals, we apply this method to identify a set of around 1 million SNPs that we call the "compatibility" panel, which has been effectively assayed in a large fraction of ancient human DNA experiments published to date. We also identify a subset of these SNPs, the "compatibility-HO" panel, which are restricted to positions that have been assayed in more than 10,000 modern people from more than 1000 diverse populations using the Affymetrix Human Origins (HO) genotyping array. The compatibility panel reduces spurious *Z*-scores owing to differing sequencing platforms by nearly an order of magnitude, while retaining ~60%–85% of statistical power for *f*-statistic analysis. We also provide a tool for users to select different tradeoffs between bias and power as well as sequencing platforms for their specific analyses.

[Supplemental material is available for this article.]

The number of ancient individuals with genome-wide ancient DNA data has expanded exponentially over the past decade and a half (Mallick et al. 2024). These data sets, which crossed the threshold of 10,000 humans with genome-wide data in 2024, have offered granular insights into ancient population history and cultural practices and have also enabled the detection of natural selection through time-series analysis (Mathieson and Terhorst 2022; Akbari et al. 2026). The increase in sample size has been turbo-charged by in-solution enrichment for targeted subsets of more than 1 million single-nucleotide polymorphisms (SNPs) informative about history and biology, which reduces the required amount of DNA sequencing by one to two orders of magnitude per individual. As of September 2025, the main in-solution SNP enrichment methods used in the field are the "Agilent 1240 k reagent" (AG), accounting for about 65% of all published individuals, and the "Twist Ancient DNA" assay (Twist or TW), accounting for 5% of published individuals. Although in-solution enrichment has greatly decreased the cost of ancient DNA analysis, these methods have the drawback that they are more prone to biases toward one allele or another at analyzed positions, and they yield more variable coverage across targeted SNPs compared with the approach of shotgun sequencing without an enrichment step (Rohland et al. 2022). These differences have meant that in coanalysis of data produced using different technological platforms, individuals with data produced using the same platform often share alleles at an elevated rate with each other, leading to false-positive inferences of shared ancestry. As a result of these biases, many researchers have restricted many of their analyses to individuals sequenced with the same technology. But because key individuals have been analyzed using different technologies, such restriction significantly limits the scientific questions that can be asked. Data sets from ancient individuals also tend to share alleles at a higher rate compared with modern individuals, not because of more shared ancestry but instead because of the propensity of ancient DNA methods to better capture some alleles than others, making it difficult to coanalyze modern and ancient individuals (Rohland et al. 2022).

Different approaches have been suggested for combining data sequenced using different technologies. A first approach consists of using imputed data (Martiniano et al. 2017; Sousa da Mota et al. 2023). Imputation works by copying haplotype segments from a reference panel and then selecting the path that best represents the sequencing data. By copying segments from an external panel, this method can leverage neighboring sites to correct for local biases that are caused by sequencing. This method has been effectively used to increase the power to discover signals of directional selection in a data set comprising thousands of individuals sequenced with various sequencing platforms (Akbari et al. 2026). However, the approach is restricted to individuals with sufficient sequencing depth (>0.5× genome-wide coverage) and requires the individual's haplotype variation to be well represented in the reference panel (Sousa da Mota et al. 2023). A second approach focuses on selecting a subset of SNPs that are unbiased across technologies. By selecting SNPs in which the ratio of reads mapping to the reference allele at heterozygous sites differed by <4% across technologies, one study identified a panel of SNPs comprising 42% of the original 1240 k (Rohland et al. 2022), increasing

Corresponding author: romainfournier@fas.harvard.edu, reich@genetics.med.harvard.edu
Article published online before print. Article, supplemental material, and publication date are at https://www.genome.org/cgi/doi/10.1101/gr.281262.125.

© 2026 Fournier et al. This article is distributed exclusively by Cold Spring Harbor Laboratory Press for the first six months after the full-issue publication date (see https://genome.cshlp.org/site/misc/terms.xhtml). After six months, it is available under a Creative Commons License (Attribution-NonCommercial 4.0 International), as described at http://creativecommons.org/licenses/by-nc/4.0/.

36:1818–1824 Published by Cold Spring Harbor Laboratory Press; ISSN 1088-9051/26; www.genome.org

Downloaded from genome.cshlp.org on November 17, 2026 . Published by Cold Spring Harbor Laboratory Press

coanalyzability but greatly reducing the number of SNPs and power of downstream analyses. The previously reported SNP panel was also not optimized to remove SNPs that show bias relative to data sets of modern individuals, making coanalysis of modern and ancient individuals with this panel unreliable (Pickrell et al. 2012). Third, SNP loadings in principal component analysis (PCA) have been used to identify sites that contribute to significant biases in some principal components (PCs). This approach requires careful processing to disentangle true ancestral components that are confounded with the sequencing platforms from technical artifacts, but it offers a practical way of performing clustering on a given data set (Margaryan et al. 2020). Finally, novel tools for preprocessing paleogenomes have been introduced to reduce reference bias. These methods require FASTQ files to be publicly available, which limits their applicability to some legacy data sets (Koptekin et al. 2025).

In this work, we introduce a method that improves upon the previous approach (Rohland et al. 2022). First, we detect biased SNPs on autosomes using an increased sample size, leveraging more than 18,000 individuals with more than 1× coverage and published genotypes, compared with fewer than 500 for the previously reported coanalysis SNP panel. Second, we use a different statistical test that accounts for the variance in read counts and does not require the same individuals to be sequenced on different technologies. Third, the statistical test generalizes to an arbitrary number of analysis platforms, and we leverage this to report a "compatibility" SNP panel that allows unbiased coanalysis of ancient and modern DNA data generated using AG, Twist, low-coverage shotgun (SG), or diploid sequencing platforms. We also identify a subset of these SNPs that are targeted by the Affymetrix Human Origins (HO) genotyping array, the "compatibility-HO" panel and that we verify as producing coanalyzable data between modern and ancient data.

Results

Annotating SNPs based on the strength of evidence for incompatibility across platforms

To identify SNPs for the compatibility panel, we started with autosomal SNPs from the 2M SNP set introduced by (Rohland et al. 2022) and then removed SNPs based on a series of criteria. First, we removed 26,385 SNPs that were not polymorphic in The 1000 Genomes Project (1KGP) (The 1000 Genomes Project Consortium 2015) or gnomAD (Chen et al. 2024) data sets. Next, we divided the individuals with sufficient coverage for imputation (coverage > 1×) from our internal database by their sequencing technology (Table 1). We leveraged haplotypes to identify sites that are likely to be heterozygous (imputation genotype posterior > 0.9) and looked for sites in which the read counts did not match this status. To achieve this, we compiled the total read count on each allele for each technology (Supplemental Table S1) and calculated a Bayes factor to assess if the proportion of reads mapping to each allele is independent of the sequencing technology (see Methods) (Supplemental Note). We ran these annotations using all technologies listed in Table 1 for our default panel (Supplemental Table S2) or restricting to technologies used to sequence ancient individuals (Supplemental Table S3). Additionally, we annotated the SNPs targeted by the Affymetrix HO array based on their relative mismatch rate between sequencing and genotyping data (see Methods) (Supplemental Table S4).

We iteratively removed SNPs with the highest bias from the 2M set and then quantified the remaining bias by computing an f_4 statistic on individuals who were assessed using two different technologies and whose genotypes were not used during the construction of the panels (Supplemental Table S5):

$$\text{bias} = f_4(\text{ind}_1\text{tech}_1, \text{ind}_1\text{tech}_2, \text{ind}_2\text{tech}_1, \text{ind}_2\text{tech}_2). \quad (1)$$

Figure 1A illustrates this remaining bias across different panel sizes. The number of retained SNPs determines the trade-off between statistical power and residual bias in the panel. For the compatibility panel, we retained SNPs with a Bayes factor greater than one, corresponding to SNPs in which our approximate model favors the hypothesis of no bias. The remaining bias at various thresholds is depicted in Figure 1A. We also provide a strict compatibility panel, retaining only SNPs with a Bayes factor greater than three (Supplemental Fig. S1). The same threshold was used to build ancient-specific compatibility panels (Table 1). Unless specified otherwise, the compatibility panel refers to the panel inferred using all technologies.

Next, we used individuals with both shotgun sequencing and HO genotyping data and annotated each SNP of the HO assay based on the relative mismatch rate between the genotypes obtained from the different technologies (Methods). Using individuals from the HGDP data set not used to compute the mismatch rates (Supplemental Table S5), we calculated the remaining bias using Equation 1. We stopped removing SNPs when the magnitude of the bias reached zero on the 1KGP individuals used for annotating the SNPs, corresponding to 20% of discarded SNPs. At this threshold, there was an 80% reduction of the bias in the held-out HGDP data set (Fig. 1B). The list of SNPs included in the default compatibility panel is available in Supplemental Table S9 and the various other versions in Supplemental Tables S10–S16.

Table 1. Summary of technologies and sample sizes used in constructing the compatibility panels

Technology	No. of individuals	Minimum coverage on 1240 k	Ancient panel (886,019 SNPs)	General panel (779,193 SNPs)
AG	7879	1×	Yes	Yes
SG	2686	1×	Yes	Yes
TW	7237	1×	Yes	Yes
Diploid shotgun genomes (ancient + modern)	424	1×	No	Yes

For each technology, we report the number of individuals analyzed and the minimum required coverage for inclusion in the data set. Summary statistics regarding the number of reads mapping to reference and alternate alleles at each locus are in Supplemental Table S1. The last two columns specify the technologies used for building the ancient and general panels. The number of SNPs refers to the autosomal SNPs present in the default panels.

Downloaded from genome.cshlp.org on November 17, 2026 . Published by Cold Spring Harbor Laboratory Press

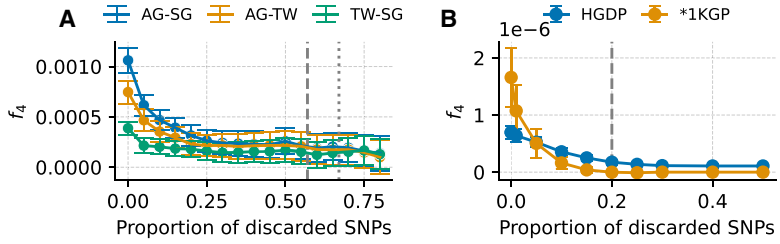

Figure 1. Selection of a threshold for inclusion in the general compatibility panels. (*A*) Bias, as defined by Equation 1, for individuals whose genotypes were not used to build the compatibility panels and sequenced using at least two technologies among AG, TW, and SG. The average value of the f_4 statistics and 1.96 × SEM are displayed. Vertical dashed and dotted lines indicate thresholds for the compatibility panel and strict compatibility panel, respectively. (*B*) Same quantity for individuals sequenced and genotyped in the Affymetrix Human Origins Array. The individuals from 1KGP were used for the SNP annotation, whereas the HGDP ones provide true out-of-sample validation.

Properties of the compatibility panel

We compared the original and unbiased SNP panels with regard to a series of metrics relevant to population genetic analysis.

We first calculated the fraction of SNPs intersecting the classic 1240 k set. For the default panels, we only observed a mild difference between the original fraction, 0.61, and the new value, 0.63. For the strict panels, however, this proportion rose to 0.70, a significant overrepresentation of these SNPs ($P < 10^{-5}$) (Supplemental Table S6). Second, we compared the minor allele frequency (MAF) spectra of both panels using individuals labeled with African (Fig. 2A) or European (Fig. 2B) ancestry. In both instances, we observed an underrepresentation of SNPs with low MAF (under ~15%) among the discarded SNPs. This plausibly reflects the fact that fewer individuals are heterozygous at these sites and that the imputation genotype posterior tends to be lower for rare variants, leading to fewer reads available to detect bias for these SNPs. Third and finally, we compared the distribution of mutation profiles, noticing a depletion of transitions in the discarded SNPs (Fig. 2C). This might reflect lower imputation genotype posterior probabilities owing to postmortem degradation, which would be expected to reduce the number of individuals passing the filtering criteria at these loci. Alternatively, it could reflect systematic differences in the allele frequency spectra of transitions and transversions in the 2M SNP set, for example, because of GC-biased gene conversion, or reflect that the ascertainment of SNPs for the HO subcomponent of the 2M SNP panel was not random with respect to allelic classes that were more or less efficient to design with the genotyping technology (Patterson et al. 2012).

Minimal technical bias in practical settings

We evaluated the bias reduction provided by our SNP panels in realistic scenarios. To achieve this, we calculated three f_4(pop1, pop2; pop3, pop4) statistics that are not expected to differ significantly from zero given the relationships among these groups. In each of the three f_4 symmetry tests, populations 1 and 3 included only AG data, whereas populations 2 and 4 consisted of data sequenced using the same alternative technology (Twist, Shotgun, Diploid Modern, or HO). This setup corresponds to a worst-case scenario, in which any technology-specific biases can be expected to lead to a particularly significant deviation from zero. Indeed, all f_4 tests produced results significantly different from zero in this setting (Z-score > 8.7) (Table 2). Using the recommended SNP panel to compute these f_4 statistics showed up to an order of magnitude reduction in the Z-scores, with the remaining Z-scores reaching values below what is typically reported in such analyses ($Z < 3$). These values are even lower when we used strict compatibility panels. In these cases, no Z-score was nominally significant (Table 2). In real analyses, a more uniform distribution of the sequencing technologies across the populations would decrease the bias. Overall, these results suggest that our proposed SNP panels effectively reduce biases.

This compatibility panel is also valuable for downstream analyses. For instance, tools like qpAdm rely on f_4 statistics to model admixture history and proportions (Haak et al. 2015). Technological biases in these statistics, however, can lead to spurious rejections of valid admixture hypotheses. To illustrate the issue, we tried to model an individual with SG data as a mixture of DG and AG individuals, with "right populations" containing individuals studied with a mixture of these three technologies. More specifically, we modeled a shotgun-sequenced Late Neolithic Spanish individual, san216.SG (Valdiosera et al. 2018), as a mixture of Oberkassel-cluster/Northwest European Mesolithic ancestry represented by a 1240 *k*–sequenced individual from the Netherlands, SPI001.AG (Olalde et al. 2026), and a diploid-called, shotgun-sequenced Neolithic Anatolian individual, I1583.DG (Mathieson et al. 2015; Gokhman et al. 2020). Our set of "right populations" consisted of a diploid-called, shotgun-sequenced Mota individual from Ethiopia, I5950.DG (Llorente et al. 2015; Lipson et al. 2022); a shotgun-sequenced Paleolithic Siberian Mal'ta individual, Russia_MA1_UP.SG (Raghavan et al. 2014); a diploid-called, shotgun-sequenced Mesolithic Ukrainian individual, I1734.DG (Mathieson et al. 2018); and an Epipaleolithic Anatolian individual from Pinarbasi, ZBC.AG (Feldman et al. 2019).

We found that when using the full 1240 k SNP set, this model is rejected ($P < 0.005$); however, when using the compatibility SNP

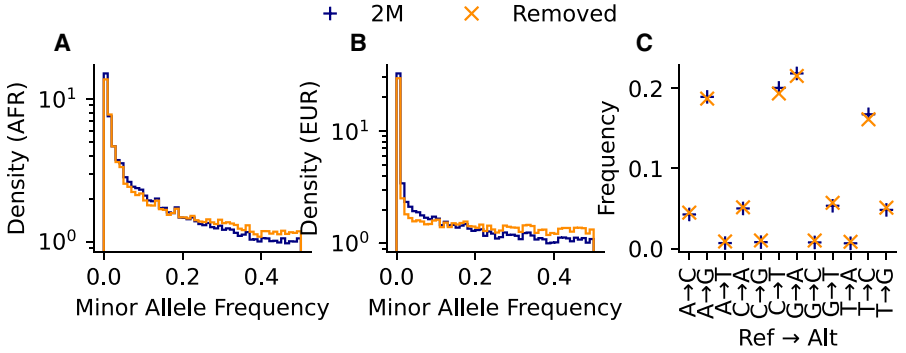

Figure 2. Properties of the compatibility panel SNPs. (*A*,*B*) Minor allele frequency spectrum in the 1KGP AFR (*A*) and EUR (*B*) continental labels. (*C*) Distribution of the mutation profiles in the 2M and compatibility panels.

Downloaded from genome.cshlp.org on November 17, 2026 . Published by Cold Spring Harbor Laboratory Press

Table 2. f_4 statistics obtained using the original and new SNP panels

				Z(General)		Z(Specific)	
Tech 1	Tech 2	N(tot)	Z(2M)	Default	Strict	Default	Strict
AG	TW	91	10.8	1.6	0.9	2.0	1.5
AG	SG	114	12.2	0.8	0.4	0.7	−0.1
AG	Modern	266	11.3	2.4	2.3	2.6	1.9
AG	HO	111	8.7	0.7	0.7	0.6	−0.3

Data from different technologies were used to calculate f_4 statistics between different groups. AG-TW, f_4 (England Neolithic TW, $n=16$; England Neolithic AG, $n=25$; Yamnaya TW, $n=25$; Yamnaya AG, $n=25$); AG-SG, f_4 (England Medieval AG, $n=65$; England Medieval SG, $n=8$; Denmark Medieval AG, $n=14$; Viking SG, $n=27$); AG-Modern, f_4 (YRI, $n=101$; Kenya Makwasinyi AG, $n=10$; GBR, $n=90$; England Medieval AG, $n=65$); and AG-HO, f_4 (Kenya Makwasinyi AG, $n=10$; Kikuyu HO, $n=4$; Belgium Medieval AG, $n=36$; French H, $n=61$). We used the default and strict compatibility panels to calculate the Z-score (general), together with panels specifically built for each pair of technologies (the ancient panel for the first two rows, and the AG-Modern for the last two). The last row shows data further restricted to the HO compatible sites, as described in the main text.

sets, we cannot reject the model ($P>0.18$ for the ancient SNP set and $P>0.36$ for the strict ancient SNP set). The standard errors around the admixture proportions are similarly small for all three SNP sets (±4.6% for 1240 k, ±5.0% for the compatibility SNP set, and ±5.3% for the strict compatibility SNP set), suggesting that the failure to reject the model is not caused by a loss of statistical power from a reduced number of SNPs. Although the inferred admixture proportions are not significantly different across the panels, it is interesting to note an increased proportion attributed to the AG source (~26.5% for the 1240K SNP set, ~29.0% for the compatibility SNP set, and ~28.4% for the strict compatibility SNP set), a shift that we would expect when the technical bias between the source and target is reduced.

Finally, we assessed how the compatibility panel affects analyses beyond f_4 statistics. We projected 159 ancient individuals with both AG and SG data onto PCs computed using modern West Eurasian populations (Methods) (Supplemental Table S7). We then calculated the mean difference between the two projections of each individual for each of the PCs (Supplemental Fig. S2). When the original HO SNP set was used, we observed significant biases in PCs 1, 3, 4, and 5 ($P=4.4\times10^{-4}$, 1.9×10^{-2}, 2.8×10^{-5}, and 8.5×10^{-3}, respectively). The bias was no longer significant using the compatibility SNP set for these PCs.

Minimal reduction in statistical power from use of the compatibility panel

We quantified the reduction in statistical power resulting from the lower number of SNPs in the compatibility panel. To perform this computation, we re-examined a data set of 291 individuals assigned to different groups across Iron Age Britain (Patterson et al. 2022). Following the original study, we first tested for differences in ancestry between pairs of groups by calculating statistics of the form f_4(group 1, group 2; Turkey Neolithic, Old Steppe), restricting to the pairs of groups with Z-scores above three in the original study. We calculated this quantity using both the original 1240 k panel and our compatibility panels. We then fit a regression line between these points and observed a regression coefficient of 0.74 for the compatibility panel and 0.81 for the ancient-specific one (Fig. 3A). The same analysis performed for the restricted version of these panels led to similar regression coefficients (Supplemental Fig. S3).

We analyzed statistics of the same form, but replacing British Iron Age groups with British Iron Age individuals, to assess how coverage impacts the standard errors of the f_4 statistics. To do so, we calculated f_4(ind 1, ind 2; Turkey Neolithic, Old Steppe) for pairs of individuals belonging to pairs of groups that were detected as being significantly different in their ancestry in the original study (reported absolute Z-scores above three). For each pair, we recorded the number of overlapping SNPs, as well as the Z-scores obtained when calculating the f_4 statistics with the new and original panels. We then split all results according to the number of overlapping sites, creating 10 sets of the same size. Within each group, we estimated the regression coefficient of the Z-scores calculated on both panels, as we did in the previous analysis (see Methods). The regression coefficient (Fig. 3B) stays at 0.85 for individuals with coverage >0.8× before progressively dropping to 0.65. The greater loss of power for lower-coverage individuals reflects the fact that for such individuals, there is expected to be little linkage

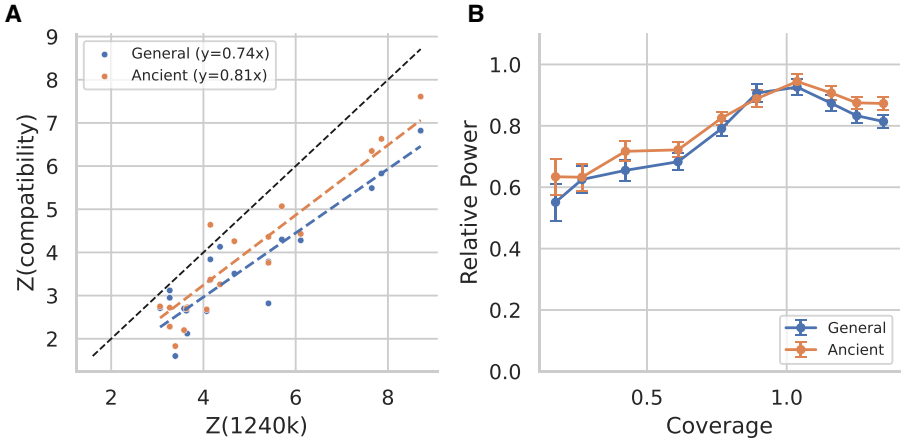

Figure 3. Power reduction in the new SNP set. (*A*) Differences in Z-scores obtained using the original SNP set (1240 k) and the compatibility panels. The regression lines y = 0.74x and y = 0.81x are shown to illustrate the reduction in power of the general and ancient compatibility panels, respectively. (*B*) Same analysis but stratifying the data by coverage. The relative power corresponds to the regression coefficient fitted on Z(compatibility) = a Z(1240 k). Error bars correspond to the 95% CI around the parameter a, assuming independent Z-scores (Methods).

Downloaded from genome.cshlp.org on November 17, 2026 . Published by Cold Spring Harbor Laboratory Press

disequilibrium among SNPs for which data are available, and hence, nearby SNPs are not filling in information gaps as is the case for higher-coverage individuals.

Discussion

We released compatibility panels, which are a subset of a previously described "2M" panel consisting of the union of positions targeted by the AG and Twist assays, along with SNPs that were effectively captured using either of these assays owing to being within 50 bp of targeted positions, as well as 15 multiallelic SNPs and six indels (Rohland et al. 2022). The default compatibility panel comprises 779,193 autosomal SNPs, to which we added the unfiltered 63,994 positions on the X Chromosome and 199,881 positions on the Y Chromosome from the 2M panel.

By reducing biases across technologies, our curated SNP panels can be used for multiple downstream analyses. One application is preserving compatibility with data generated using earlier sequencing technologies. As a result, new individuals can be analyzed without needing to match the platforms used in previous studies. Second, the panels enable joint modeling of ancient and modern individuals in f_4-based methods, such as qpAdm and qpWave (Reich et al. 2012; Haak et al. 2015). Finally, methods beyond f_4 statistics may benefit from the curated panels. This is particularly relevant for frequency-based approaches and PCAs, in which platform-specific biases can lead to spurious results.

A limitation of our model is that reads are treated as independent entities. This prevents strict probabilistic interpretation of the annotations and requires relying on external validation sets to test the panels, as done in this analysis. As more individuals become publicly available, allowing for the use of individual read counts, a mixed model accounting for individual-level effects could increase the power of the compatibility panels. Next, the power to detect technology-specific bias is directly linked to the number of heterozygous individuals sequenced at each locus. As a result, our method is underpowered to detect problematic SNPs that have MAFs under 10% or that are only present in underrepresented ancestries. An important caveat is that the new SNP panel, despite significantly reducing bias, does not fully eliminate it. Therefore, we recommend that analysts be cautious when interpreting Z-scores that are close to the rejection threshold. Finally, the compatibility panel has nonhomogeneous coverage across technologies. For some analyses, it might be valuable to impose a further coverage threshold on the remaining SNPs.

As larger and more diverse data sets become available, future updates of this panel could further reduce biases. We also release a script and current read counts that researchers can use to build their own compatibility panel. For example, if residual inflation in Z-scores is observed, analysts can further reduce the number of SNPs in the compatibility panel, create a panel restricted to the technologies present in their analysis, or generate a population-specific panel by only using reads from individuals in relevant populations. For convenience, the package contains the lists obtained for common pairs of technologies and various thresholds, in addition to the recommended ones.

For some analyses, the panels we provide will not be useful. Whole-genome sequencing remains critical for applications such as de novo SNP discovery, methylation studies, and structural variant detection. Whole-genome sequencing can also improve resolution for applications that use capture data but benefit from higher SNP density like the detection of IBD segments, demographic inference, and selection scans. However, for these latter analyses, the greatly increased sample sizes accessible from capture data makes it critical to have methodologies that reliably allow coanalysis of capture and sequencing data.

Finally, for applications relying on modeling of nonzero f-statistics, such as building trees based on outgroup f_3-statistics, it is important to apply a coverage threshold to ensure that the same set of SNPs is being compared for each technology, as different frequency spectrums associated with the SNPs targeted by the technologies result in different expected values of nonzero statistics.

Methods

Removing SNPs based on differences in reference biases

Our analysis leverages more than 18,000 individuals (Table 1), whose genotypes were imputed using the same pipeline as that described in a recent study of natural selection (Akbari et al. 2026). We base our analysis on the GRCh37 human reference genome, which is the reference genome used for the overwhelming majority of ancient human DNA studies (Mallick et al. 2024). For each SNP in the 2M SNP panel (Rohland et al. 2022) that is polymorphic in the 1KGP or gnomAD data sets, we retained data imputed as heterozygous with a genotype posterior probability >90%. Using these individuals, we reported, for each technology, the number of reads mapping to the reference and alternate alleles (Supplemental Table S1). We then built a contingency table with sequencing technologies as rows and the number of reads mapping to the reference and alternate alleles as columns. For each SNP, we calculated a Bayes factor assessing the independence of each row (Supplemental Note). We provide panels for two distinct thresholds, a Bayes factor of one and three. Although these numbers are commonly used in the literature and worked well in our tests, users can apply different thresholds using our Python package. Annotations for the default and ancient-specific panels are available in Supplemental Tables S2 and S3, respectively. Compatibility panels used in the paper are available in Supplemental Tables S9 (default panel) through S16.

Removing SNPs for the compatibility-HO panel

We leveraged 1028 individuals with both sequencing and genotyping data (Patterson et al. 2012; Lazaridis et al. 2014; Prüfer et al. 2014; Mallick et al. 2016; Skoglund et al. 2016; Nakatsuka et al. 2017; Fan et al. 2019; Bergström et al. 2020). For each SNP, we calculated the relative number of mismatches over the total number of heterozygous individuals at that site. We discarded SNPs according to this metric. The threshold was set to the first value for which no bias was observed in the 1KGP individuals.

Calculating f_4 statistics

We calculated f_4 statistics using *ADMIXTOOLS 2* (Maier et al. 2023) with the "maxmiss" parameter set to zero. Individuals used to assess the panels are listed in Supplemental Table S5 and can be accessed through the AADR data set (Mallick et al. 2024).

qpAdm

For faster computation, we ran qpWave/qpAdm on precomputed output from qpfstats (see https://github.com/DReichLab/AdmixTools/blob/master/qpfs.pdf) with a poplistname that has diploid modern Han Chinese (Mallick et al. 2016) as the first population to improve coverage for qpfstats; all target, source, and right populations; and the parameters" allsnps: YES, inbreed: NO."

Downloaded from genome.cshlp.org on November 17, 2026 . Published by Cold Spring Harbor Laboratory Press

PCA

We ran a PCA using smartpca (Patterson et al. 2006) with the lsqproject option set to YES. We calculated PCs using the individuals of Supplemental Table S7 with the HO and then projected the ancient individual on these axes. We then used a *t*-test to calculate *P*-values for deviation from a zero-mean difference on each component.

Power analysis

We analyzed the same set of individuals and their corresponding population labels as previously described (Supplemental Table S8; Patterson et al. 2022). We fit a linear regression without an intercept to the resulting *Z*-scores to estimate the power reduction. For the coverage analysis, we proceeded in the same way but this time using pairs of individuals belonging to the different groups with large *Z*-scores (greater than three). We separated the pairs of individuals according to the number of overlapping sites. If P denotes the proportion of overlapping sites on the 1240 k panel, and c denote the coverage, we can use a Poisson approximation to obtain

$$P \approx (1 - e^{-c})^2.$$

We inverted this relation to obtain c. This equation assumes that the probability of a SNP being missing is independent of other reads and is uniform, which means that the actual value of c is likely to be lower. In other words, the power is likely to remain higher at lower coverages than the reported 0.8×.

We fitted the regression line assuming all *Z*-scores are independent. This means that the confidence intervals provided around the slope are tighter than what is expected if points were truly independent.

Editing

We wrote a rough draft of each paragraph, and once completed, used large language models to edit at the sentence level. We typically asked for three versions of some sentences. We then selected the version we preferred, or we mixed different elements of different answers. This tool was only used to edit the style of this paper, not its structure nor its content. We then carried out multiple additional rounds of editing (not assisted by these tools).

Code availability

We released a Python package for users to create their own panels for specific use cases, available at GitHub (https://github.com/rmnfournier/compatibility-panel) and as Supplemental Code.

Competing interest statement

The authors declare no competing interests.

Acknowledgments

We thank Shop Mallick, Bárbara Sousa da Mota, Lars Fehren-Schmitz, and Nick Patterson for valuable discussions. We thank several anonymous reviewers for their constructive comments. We thank the bioinformatics team in our laboratory for making available the data sets we used for identifying SNPs susceptible to bias. This work was supported by John Templeton Foundation grant 61220, by National Institutes of Health grant HG012287, and by the Howard Hughes Medical Institute, and was partly supported by the Swiss National Science Foundation (SNSF) through a Postdoc.Mobility fellowship grant 239137 (R.F.).

Author contributions: D.R., A.P.F., and R.F. designed the study; R.F. developed and implemented the model; R.F. and D.T. analyzed the data; R.F. developed software tools; R.F. and D.R. wrote the manuscript, with input from D.T.; and D.R. supervised the work.

References

The 1000 Genomes Project Consortium. 2015. A global reference for human genetic variation. *Nature* **526:** 68–74. doi:10.1038/nature15393

Akbari A, Perry A, Barton AR, Kariminejad M, Gazal S, Li Z, Zeng Y, Mittnik A, Patterson N, Mah M, et al. 2026. Ancient DNA reveals pervasive directional selection across West Eurasia. *Nature* **654:** 419–428. doi:10.1038/s41586-026-10358-1

Bergström A, McCarthy SA, Hui R, Almarri MA, Ayub Q, Danecek P, Chen Y, Felkel S, Hallast P, Kamm J, et al. 2020. Insights into human genetic variation and population history from 929 diverse genomes. *Science* **367:** eaay5012. doi:10.1126/science.aay5012

Chen S, Francioli LC, Goodrich JK, Collins RL, Kanai M, Wang Q, Alföldi J, Watts NA, Vittal C, Gauthier LD, et al. 2024. A genomic mutational constraint map using variation in 76,156 human genomes. *Nature* **625:** 92–100. doi:10.1038/s41586-023-06045-0

Fan S, Kelly DE, Beltrame MH, Hansen MEB, Mallick S, Ranciaro A, Hirbo J, Thompson S, Beggs W, Nyambo T, et al. 2019. African evolutionary history inferred from whole genome sequence data of 44 indigenous African populations. *Genome Biol* **20:** 82. doi:10.1186/s13059-019-1679-2

Feldman M, Fernández-Domínguez E, Reynolds L, Baird D, Pearson J, Hershkovitz I, May H, Goring-Morris N, Benz M, Gresky J, et al. 2019. Late Pleistocene human genome suggests a local origin for the first farmers of central Anatolia. *Nat Commun* **10:** 1218. doi:10.1038/s41467-019-09209-7

Gokhman D, Nissim-Rafinia M, Agranat-Tamir L, Housman G, García-Pérez R, Lizano E, Cheronet O, Mallick S, Nieves-Colón MA, Li H, et al. 2020. Differential DNA methylation of vocal and facial anatomy genes in modern humans. *Nat Commun* **11:** 1189. doi:10.1038/s41467-020-15020-6

Haak W, Lazaridis I, Patterson N, Rohland N, Mallick S, Llamas B, Brandt G, Nordenfelt S, Harney E, Stewardson K, et al. 2015. Massive migration from the steppe was a source for Indo-European languages in Europe. *Nature* **522:** 207–211. doi:10.1038/nature14317

Koptekin D, Yapar E, Vural KB, Sağlıcan E, Altınışık NE, Malaspinas A-S, Alkan C, Somel M. 2025. Pre-processing of paleogenomes: mitigating reference bias and postmortem damage in ancient genome data. *Genome Biol* **26:** 6. doi:10.1186/s13059-024-03462-w

Lazaridis I, Patterson N, Mittnik A, Renaud G, Mallick S, Kirsanow K, Sudmant PH, Schraiber JG, Castellano S, Lipson M, et al. 2014. Ancient human genomes suggest three ancestral populations for present-day Europeans. *Nature* **513:** 409–413. doi:10.1038/nature13673

Lipson M, Sawchuk EA, Thompson JC, Oppenheimer J, Tryon CA, Ranhorn KL, Luna D, Sirak KM, Olalde KA, Ambrose I, et al. 2022. Ancient DNA and deep population structure in sub-Saharan African foragers. *Nature* **603:** 290–296. doi:10.1038/s41586-022-04430-9

Llorente MG, Jones ER, Eriksson A, Siska V, Arthur KW, Arthur JW, Curtis MC, Stock JT, Coltorti M, Pieruccini P, et al. 2015. Ancient Ethiopian genome reveals extensive Eurasian admixture in Eastern Africa. *Science* **350:** 820–822. doi:10.1126/science.aad2879

Maier R, Flegontov P, Flegontova O, Işıldak U, Changmai P, Reich D. 2023. On the limits of fitting complex models of population history to *f*-statistics. *eLife* **12:** e85492. doi:10.7554/eLife.85492

Mallick S, Li H, Lipson M, Mathieson I, Gymrek M, Racimo F, Zhao M, Chennagiri N, Nordenfelt S, Tandon A, et al. 2016. The Simons Genome Diversity Project: 300 genomes from 142 diverse populations. *Nature* **538:** 201–206. doi:10.1038/nature18964

Mallick S, Micco A, Mah M, Ringbauer H, Lazaridis I, Olalde I, Patterson N, Reich D. 2024. The Allen Ancient DNA resource (AADR) a curated compendium of ancient human genomes. *Sci Data* **11:** 182. doi:10.1038/s41597-024-03031-7

Margaryan A, Lawson DJ, Sikora M, Racimo F, Rasmussen S, Moltke I, Cassidy LM, Jørsboe E, Ingason A, Pedersen MW, et al. 2020. Population genomics of the Viking world. *Nature* **585:** 390–396. doi:10.1038/s41586-020-2688-8

Martiniano R, Cassidy LM, Ó'Maoldúin R, McLaughlin R, Silva NM, Manco L, Fidalgo D, Pereira T, Coelho MJ, Serra M, et al. 2017. The population genomics of archaeological transition in west Iberia: investigation of ancient substructure using imputation and haplotype-based methods. *PLoS Genet* **13:** e1006852. doi:10.1371/journal.pgen.1006852

Mathieson I, Terhorst J. 2022. Direct detection of natural selection in Bronze Age Britain. *Genome Res* **32:** 2057–2067. doi:10.1101/gr.276862.122

Downloaded from genome.cshlp.org on November 17, 2026 . Published by Cold Spring Harbor Laboratory Press

Mathieson I, Lazaridis I, Rohland N, Mallick S, Patterson N, Roodenberg SA, Harney E, Stewardson K, Fernandes D, Novak M, et al. 2015. Genome-wide patterns of selection in 230 ancient Eurasians. *Nature* **528:** 499–503. doi:10.1038/nature16152

Mathieson I, Alpaslan-Roodenberg S, Posth C, Szécsényi-Nagy A, Rohland N, Mallick S, Olalde I, Broomandkhoshbacht N, Candilio F, Cheronet O, et al. 2018. The genomic history of southeastern Europe. *Nature* **555:** 197–203. doi:10.1038/nature25778

Nakatsuka N, Moorjani P, Rai N, Sarkar B, Tandon A, Patterson N, Bhavani GS, Girisha KM, Mustak MS, Srinivasan S, et al. 2017. The promise of discovering population-specific disease-associated genes in south Asia. *Nat Genet* **49:** 1403–1407. doi:10.1038/ng.3917

Olalde I, Altena E, Bourgeois Q, Fokkens H, Amkreutz L, Baetsen S, Deguilloux M-F, Fichera A, Flas D, Gandini F, et al. 2026. Lasting lower Rhine–Meuse forager ancestry shaped Bell Beaker expansion. *Nature* **652:** 938–946. doi:10.1038/s41586-026-10111-8

Patterson N, Price AL, Reich D. 2006. Population structure and eigenanalysis. *PLoS Genet* **2:** e190. doi:10.1371/journal.pgen.0020190

Patterson N, Moorjani P, Luo Y, Mallick S, Rohland N, Zhan Y, Genschoreck T, Webster T, Reich D. 2012. Ancient admixture in human history. *Genetics* **192:** 1065–1093. doi:10.1534/genetics.112.145037

Patterson N, Isakov M, Booth T, Büster L, Fischer C-E, Olalde I, Ringbauer H, Akbari A, Cheronet O, Bleasdale M, et al. 2022. Large-scale migration into Britain during the middle to late bronze age. *Nature* **601:** 588–594. doi:10.1038/s41586-021-04287-4

Pickrell JK, Patterson N, Barbieri C, Berthold F, Gerlach L, Güldemann T, Kure B, Mpoloka SW, Nakagawa H, Naumann C, et al. 2012. The genetic prehistory of southern Africa. *Nat Commun* **3:** 1143. doi:10.1038/ncomms2140

Prüfer K, Racimo F, Patterson N, Jay F, Sankararaman S, Sawyer S, Heinze A, Renaud G, Sudmant PH, de Filippo C, et al. 2014. The complete genome sequence of a Neanderthal from the Altai Mountains. *Nature* **505:** 43–49. doi:10.1038/nature12886

Raghavan M, Skoglund P, Graf KE, Metspalu M, Albrechtsen A, Moltke I, Rasmussen S, Stafford TW, Orlando L, Metspalu E, et al. 2014. Upper Paleolithic Siberian genome reveals dual ancestry of native Americans. *Nature* **505:** 87–91. doi:10.1038/nature12736

Reich D, Patterson N, Campbell D, Tandon A, Mazieres S, Ray N, Parra MV, Rojas W, Duque C, Mesa N, et al. 2012. Reconstructing native American population history. *Nature* **488:** 370–374. doi:10.1038/nature11258

Rohland N, Mallick S, Mah M, Maier R, Patterson N, Reich D. 2022. Three assays for in-solution enrichment of ancient human DNA at more than a million SNPs. *Genome Res* **32:** 2068–2078. doi:10.1101/gr.276728.122

Skoglund P, Posth C, Sirak K, Spriggs M, Valentin F, Bedford S, Clark GR, Reepmeyer C, Petchey F, Fernandes D, et al. 2016. Genomic insights into the peopling of the Southwest Pacific. *Nature* **538:** 510–513. doi:10.1038/nature19844

Sousa da Mota B, Rubinacci S, Cruz Dávalos DI, G. Amorim CE, Johannsen M, Szmyt NN, Włodarczak MH, Szczepanek P, et al. 2023. Imputation of ancient human genomes. *Nat Commun* **14:** 3660. doi:10.1038/s41467-023-39202-0

Valdiosera C, Günther T, Vera-Rodríguez JC, Ureña I, Iriarte E, Rodríguez-Varela R, Simões LG, Martínez-Sánchez RM, Svensson EM, Malmström H, et al. 2018. Four millennia of Iberian biomolecular prehistory illustrate the impact of prehistoric migrations at the far end of Eurasia. *Proc Natl Acad Sci* **115:** 3428–3433. doi:10.1073/pnas.1717762115

Received July 30, 2025; accepted in revised form July 21, 2026.